Supporting Information

Elifnaz Sağlamkaya[a], Artem Musiienko[b], Mohammad Saeed Shadabroo[a], Bowen Sun[a], Sreelakshmi Chandrabose[b], Oleksandra Shargaieva[d], Giulia Lo Gerfo M.[e], Niek F. van Hulst[e,f], Safa Shoaee*[a]

a.Elifnaz Saglamkaya, Mohammad Saeed Shadabroo, Bowen Sun, Prof. Dr. S.Shoaee Disordered Semiconductor Optoelectronics, Institute of Physics and Astronomy, University of Potsdam, Karl-Liebknecht-Str. 24-25, 14476 Potsdam-Golm, Germany

E-mail: shoai@uni-potsdam.de

b. Dr. Artem Musiienko, Department Novel Materials and Interfaces for Photovoltaic Solar Cells, Helmholtz-Zentrum Berlin für Materialien und Energie, Kekuléstraße 5, 12489 Berlin, Germany

c. Elifnaz Saglamkaya, Dr. Sreelakshmi Chandrabose
Soft Matter Physics, Institute of Physics and Astronomy, University of Potsdam, Karl-Liebknecht-Str. 24-25, 14476 Potsdam-Golm, Germany

d. Dr. Oleksandra Shargaieva, Helmholtz-Zentrum Berlin für Materialien und Energie GmbH, HySPRINT Innovation Lab, Department "Solution Processing of Hybrid Materials & Devices" (SE-ALM), Kekuléstr. 5, Berlin 12489, Germany

e. Giulia Lo Gerfo M., Prof. Dr. Niek F. van Hulst
ICFO – Institut de Ciencies Fotoniques, The Barcelona Institute of Science and Technology, 08860 Castelldefels, Barcelona, Spain.

f. Prof. Dr. Niek F. van Hulst

ICREA – Institució Catalana de Recerca i Estudis Avançats, Passeig Lluís Companys 23, 08010 Barcelona, Spain

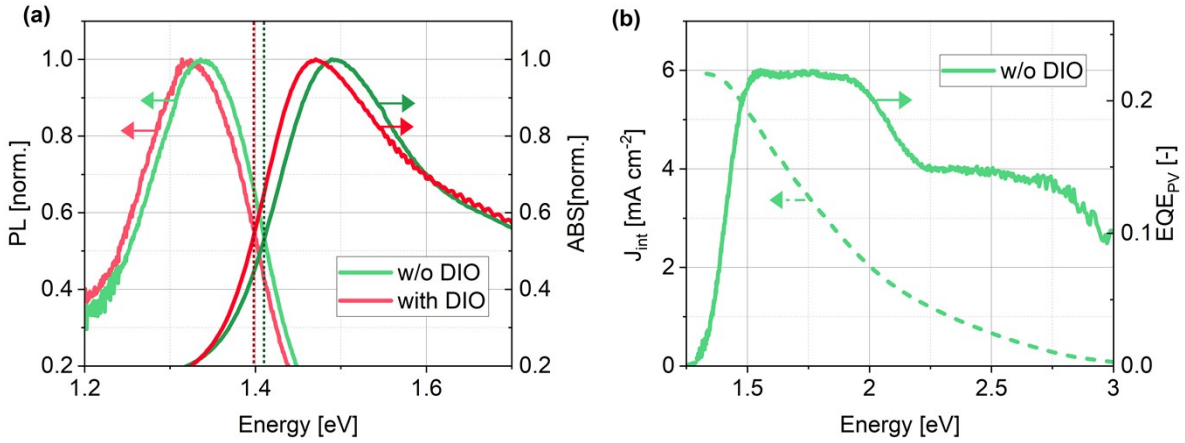

Figure S1: a. Absorption and photoluminescence (PL) spectra of 15 nm neat Y6 films with and w/o DIO additive. The crossing point of both spectra is marked with perpendicular dot line, which is placed at 1.39 eV for with DIO film and 1.41 eV for the w/o DIO film. **b.** The integrated J_{SC}, left axis, and linear photovoltaic external quantum efficiency (EQE_{PV}), right axis, of the complete devices with 100 nm active layer thickness. The J_{int} for Y6 (w/o DIO) is 5.9 $mAcm^{-2}$.

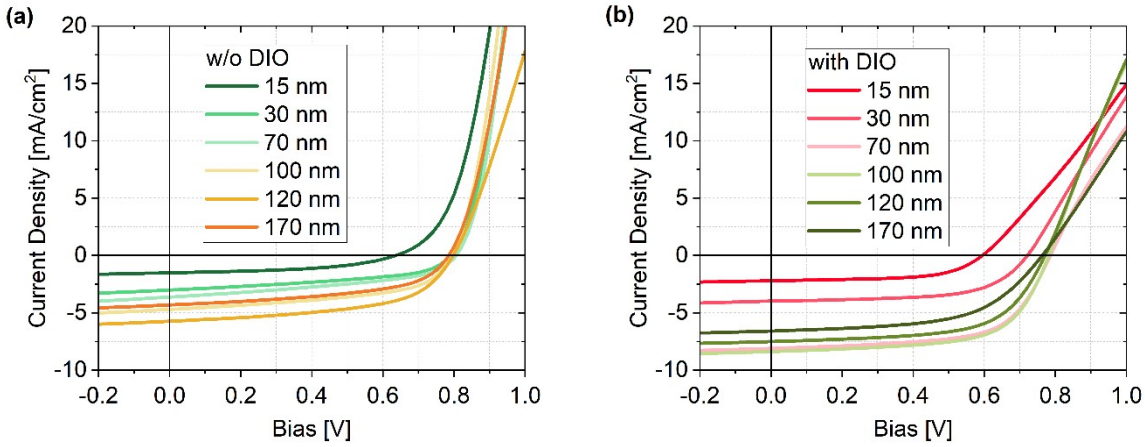

Figure S2: Current density-voltage characteristics of the Y6 devices **a.** w/o and **b.** with DIO additive with structure ITO/CuSCN/Y6/Phen-NaDPO/Al (fully reflecting 100nm) with the device area of 6 mm^2 under simulated AM1.5G light in different Y6 thicknesses from 15 nm to 170 nm.

Table S1. Photovoltaic parameters of Y6 devices with structure ITO/CuSCN/Y6/Phen-NaDPO/Al (fully reflecting 100nm) with varying thicknesses.

Device	J_{SC} **[mA cm^{-2}]**	V_{OC} **[V]**	***FF*** **[%]**	**PCE [%]**
15 nm w/o DIO	1.5	0.63	47	0.46
30 nm w/o DIO	3.0	0.78	47	1.1
70 nm w/o DIO	3.63	0.80	45	1.3
100 nm w/o DIO	4.3	0.79	51	1.7
120 nm w/o DIO	5.1	0.80	55	2.5
170 nm w/o DIO	4.2	0.78	51	1.7
15 nm with DIO	2.2	0.59	59	0.7
30 nm with DIO	4.0	0.72	61	1.7
70 nm with DIO	8.1	0.78	63	4.0

100 nm with DIO	8.3	0.78	63	4.1
120 nm with DIO	7.5	0.77	61	3.5
170 nm with DIO	6.5	0.76	56	2.8

Supplementary Note 1. Photo-Hall Measurements: The Y6 film with DIO shows a decrease in the Hall mobility with increasing illumination intensity (**Figure S3b**.). This behaviour takes place due to the increase in the density of the mobile p-type carriers, which is an observed behaviour in other systems as well.[1] As we have confirmed with the SCLC mobility measurements, Y6 with the DIO additive has balanced mobility for electrons and the holes, whereas in the no additive device the hole mobility is much smaller (see table 2). For the reason that the holes are being relatively immobile in the Y6 w/o DIO compared to the electrons, Hall mobility remains unchanged with the increasing intensity. The photoconductivity measurements revealed a longer free carrier diffusion length and life-time for the electrons in the Y6 with DIO at 1 sun equivalent illumination conditions. The carrier density can be calculated by the product of the mobiltity and the photoconductivity $\Delta N = \sigma \times \mu \times e$, for the DIO where we see the effect of both types of charge carriers, the carrier density is calculated form the double of this product. $\Delta N = 2 \times \sigma \times \mu \times e$, where e is the elementary charge, μ is mobility and is conductivity.

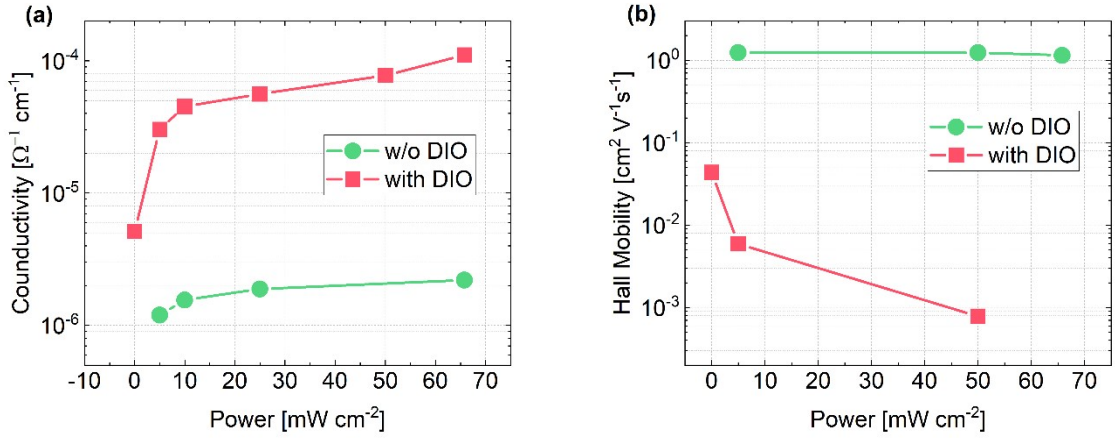

Figure S3 a. The 4-probe conductivity measurement of the 100 nm thick neat Y6 films on glass with Ag contacts under the illumination with the excitation energy of 1.7 eV. **b.** The intensity dependent Hall mobility of the same films estimated with the calculated carrier density and the conductivity.

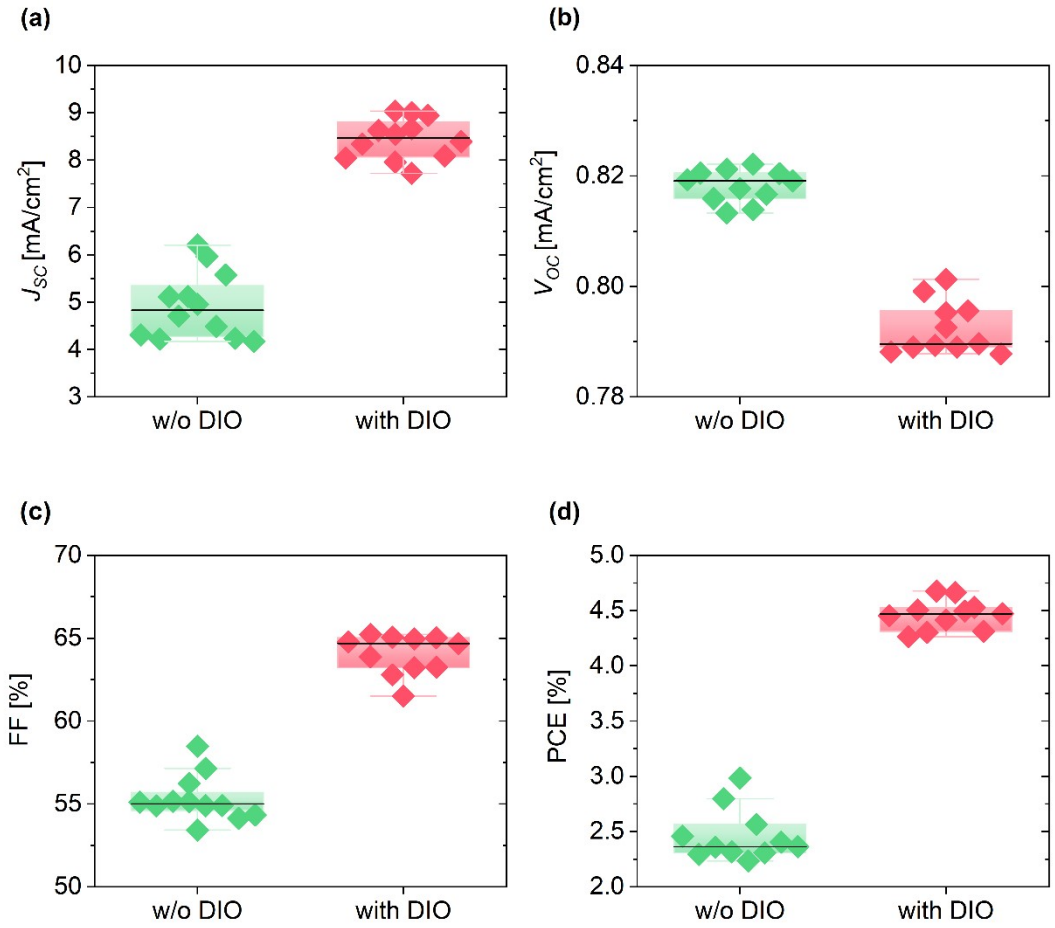

Figure S4: Photovoltaic performance parameters and cell statistics of Y6 devices with and w/o DIO with 100 nm active layer thickness with 100 nm Al contact.

Table S2. Average photovoltaic parameters and standard deviations for Y6 ($CHCl_3$, 110°C for 10 min) and Y6 ($CHCl_3$, additive DIO 0.5% v/v, 110°C for 10 min) devices with structure ITO/CuSCN/Y6/Phen-NaDPO/Al (fully reflecting 100nm). Active layer thickness is ca. 100 nm and A=6 mm^2.

Device	V_{OC} **[V]**	J_{SC} **[mAcm^{-2}]**	**FF [%]**	**PCE [%]**
w/o DIO	0.8191 ±0.003	4.8 ±0.6	55.0 ±1.3	2.363±0.23
with DIO	0.7896 ±0.004	8.4 ±0.4	64.68 ±1.2	4.471±0.13

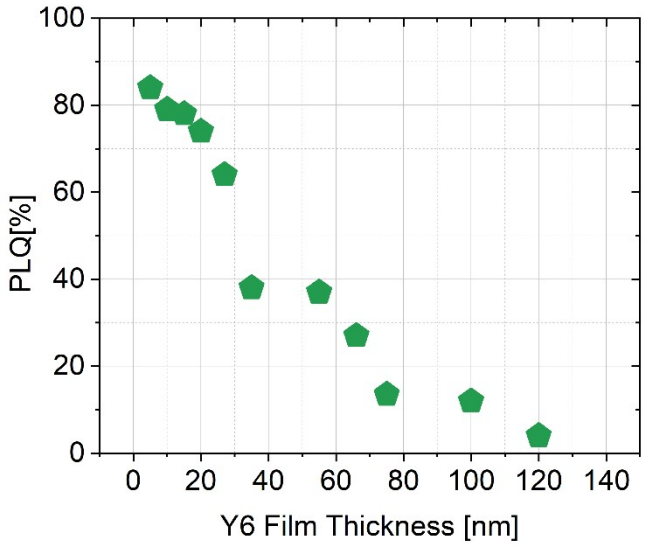

Figure S5: Photoluminescence quenching (PLQ) as a function of Y6 layer thickness (w/o DIO) of the CuSCN/Y6 bilayer films on glass. (PLQ of each bilayer is calculated with respect to the neat Y6 film on glass with the same thickness)

Supplementary Note 2. Spatially and time resolved fluorescence microscopy:

The 100 nm with and w/o DIO Y6 films were excited with ~1.55 eV energy. The 2D spatio-temporal maps were generated by integrating the collected fluorescence intensity $I(x,t)$ at every 20 ps at each scanning position (every 100 nm between 600 nm to -600 nm) along the cross-section of the excitation profile. 2D fits were performed on the whole map, the effective diffusion coefficient (D_{eff}) and τ_{eff} as the output parameters. In our case, the estimated D_{eff} is close to the value of the actual diffusion coefficient (D) since great attention was paid into the measurement conditions to avoid exciton-exciton annihilation which might cause overestimation of the D.

The 100 nm Y6 (w/o DIO) neat film has the effective exciton lifetime of 1336 ps at the excitation point which is longer than exciton lifetime of the Y6 (with DIO) of 1295 ps. On the contrary the Y6 (with DIO) film has a higher D of 0.025 cm^2/s whereas Y6 (w/o DIO) has 0.018 cm^2/s. The calculated exciton diffusion length ($L_D = \sqrt{D\tau_{eff}}$) of the Y6 (with DIO) film is 7 nm higher than the Y6 (w/o DIO) (~56 nm & 49 nm respectively) which doesn't explain significantly higher J_{SC} of the Y6 devices with DIO. [2]

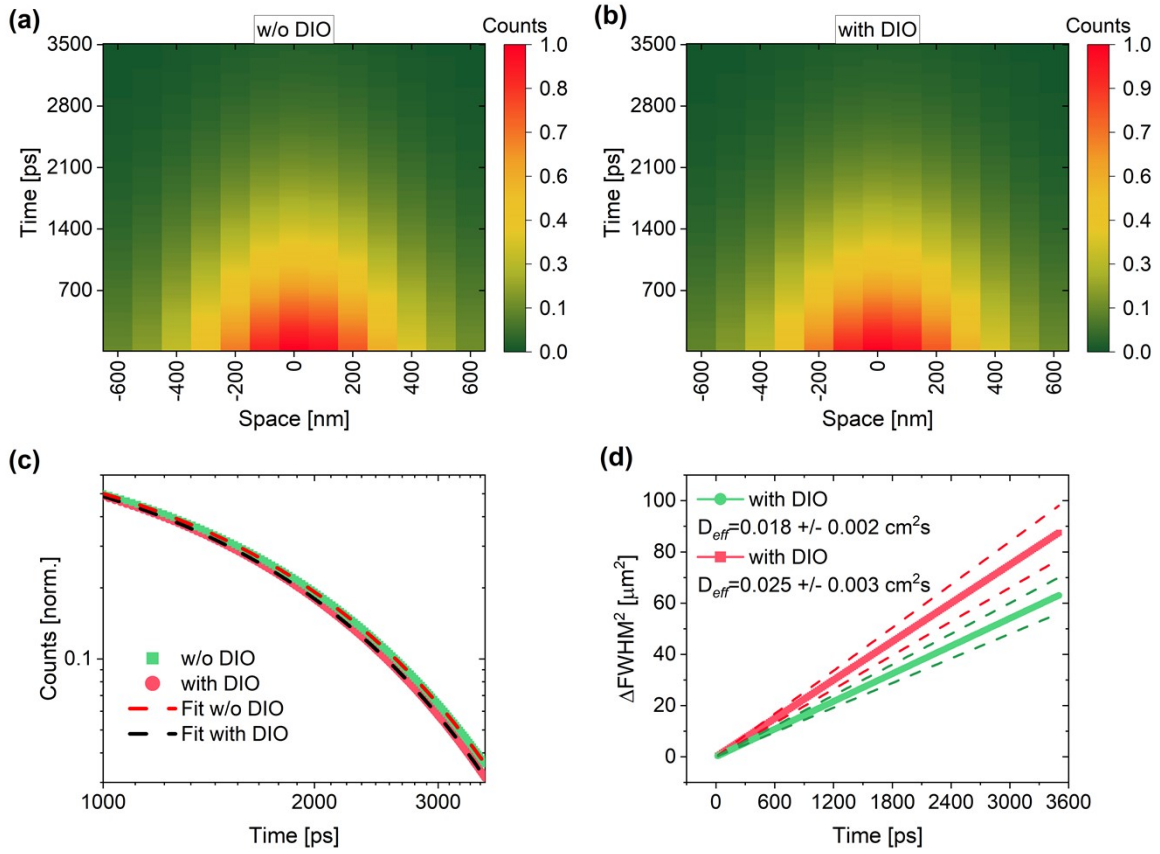

Figure S6: 2D images of the 100 nm Y6 films on glass **a.** w/o DIO and **b.** with DIO generated with the time resolve fluorescence microscopy measurement using low excitation intensity (30 nJ). The analysis of the emission over time and space give (**c.**) the exciton lifetime and (**d.**) the diffusion coefficient for the two different samples.

Supplementary Note 3. Space charge limited current (SCLC) Fittings: The mobility of the devices was calculated from the modified Mott-Gurney equation, named Murgatroyd/Gill equation (**Equation 1**) that includes the term field enhancement factor gamma (γ). In the Mott-Gurney theory[3], the current depends on voltage quadratically in the SCLC region. However, real systems usually have slightly larger slopes in the SCLC region, which could be resulted by energetic disorder and traps. [4]

$$J = \frac{9}{8}\varepsilon_r\varepsilon_0\mu_0\frac{(V - V_{bi})^2}{L^3}exp(0.891\gamma\sqrt{\frac{V - V_{bi}}{L}})$$

Equation 1

Here ε_0 is the vacuum permittivity, ε_r is the material's relative dielectric constant, L is the thickness of the active layer and the μ_0 is the mobility at 0 field.

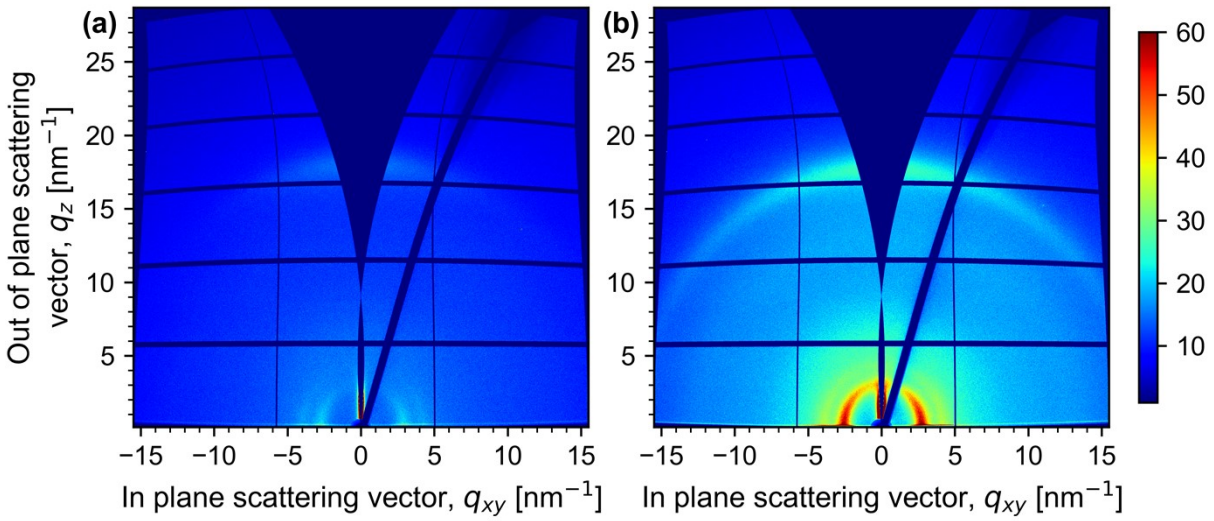

Figure S7 The 2D GIWAXS patterns of the 100 nm neat Y6 films **a.** w/o and **b.** with DIO additive on Si wafers. The film processed from the solutions with the DIO solvent additive has significantly higher long-range order.

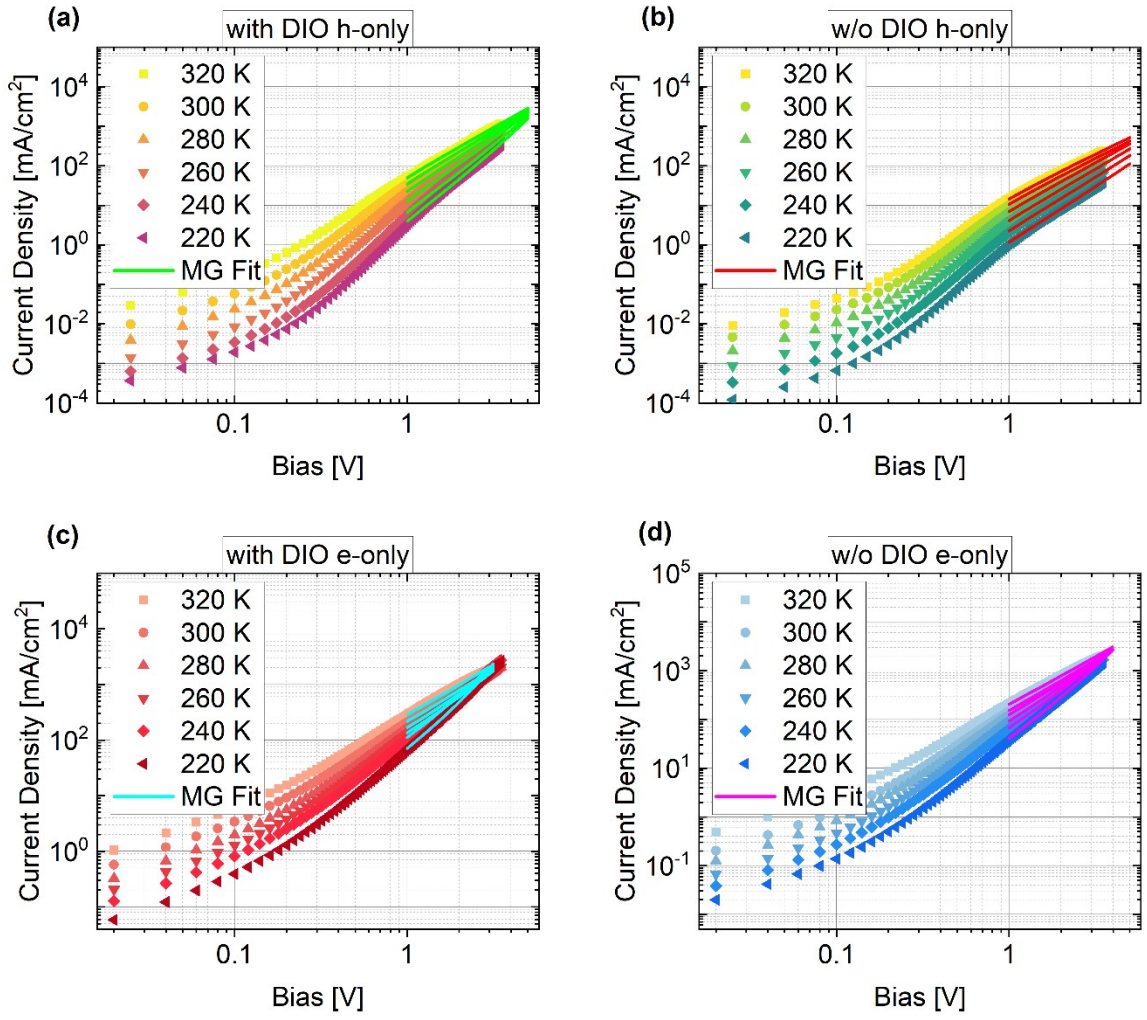

Figure S8: Space charge limited current vs. applied bias curves for the single carrier Y6 devices of hole only **a.** with DIO **b.** w/o DIO in ITO/MoO_x/Y6/ MoO_x/Ag device structure with 200 nm Y6 thickness and electron only **c.** with DIO and **d.** w/o DIO in ITO/ZnO/Y6/Phen-NaDPO/Al device structure with 170 nm Y6 thickness. Murgatroyd/Gill (MG) fittings are shown with straight lines for the experimental data range of 1-2.5 Volts.

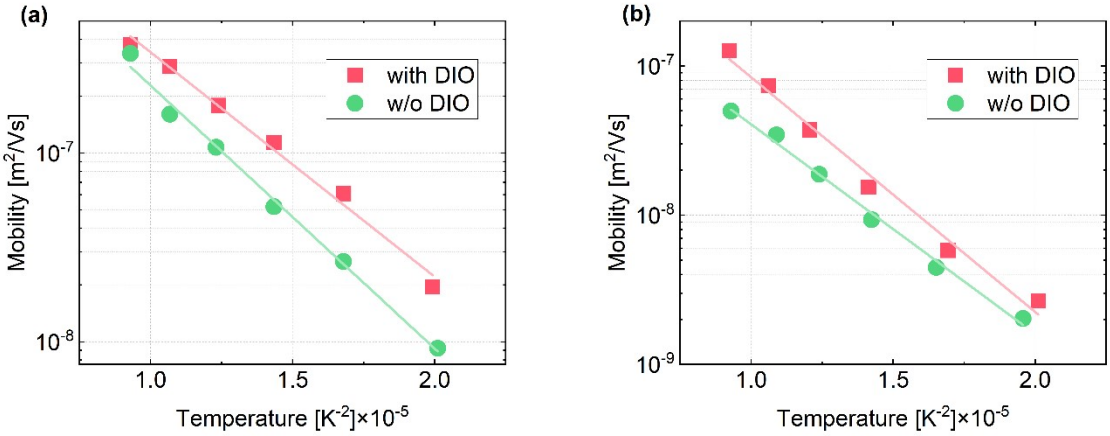

Figure S9: The temperature dependent zero field mobility of the **a.** electron only devices and **b.** hole only devices are shown, the spatial disorder was estimated from the linear fittings with the equation, $\mu_0(T) = \mu^* \times e^{(-\frac{c \times \sigma}{k_B T})}$ where $\mu_0(T)$ is the tempearature dependent mobility, μ^* is the mobility at infinite temperature, and σ is the spatial disorder.

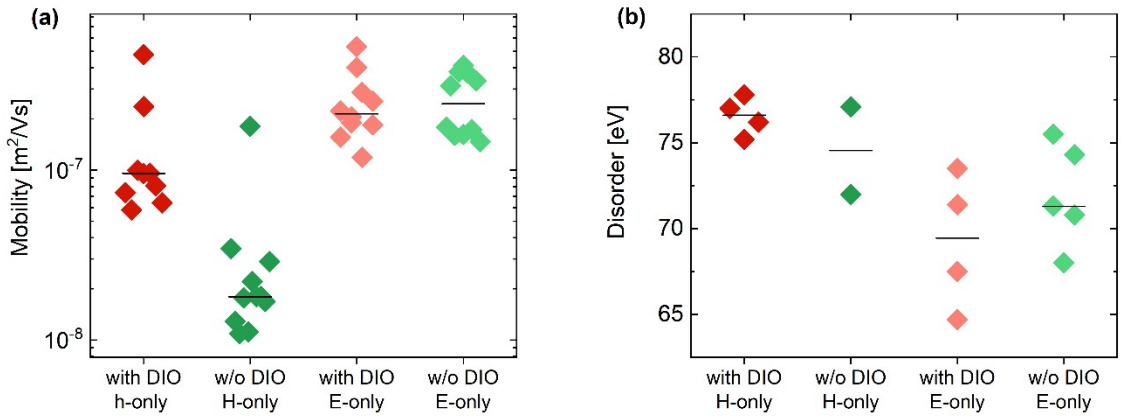

Figure S10: Average hole and electron SCLC mobility and the LUMO and HOMO energetic disorder value distributions of the both systems are shown.

Table S3. Simulation parameters of the curves that are shown in **Figure 5**.

Simulation Parameters	**w/o DIO**	**with DIO**
k_2 [$cm^3\ s^{-1}$]	1×10^{-10}	2×10^{-11}
Effective DOS VB=CB [cm^{-3}]	4.7×10^{20}	1.7×10^{21}
E_{bg} [eV]	1.4	1.4
μ_e [cm^2/Vs]	1.5×10^{-3}	1.5×10^{-3}
μ_h [cm^2/Vs]	7×10^{-4}	1.5×10^{-3}
Acceptor Defects, VB tail, Below E_c 0.7 eV [cm^{-3}]	-	1×10^{14}
Electron Affinity of the Active Layer [eV]	4.000	4.000
Electron Affinity of the ETL [eV]	4.000	4.000
Ionization Potential of the HTL [eV]	5.447	5.465
Metal Work Function of Anode [eV]	5.060	5.060
Metal Work Function of Cathode [eV]	4.000	4.050

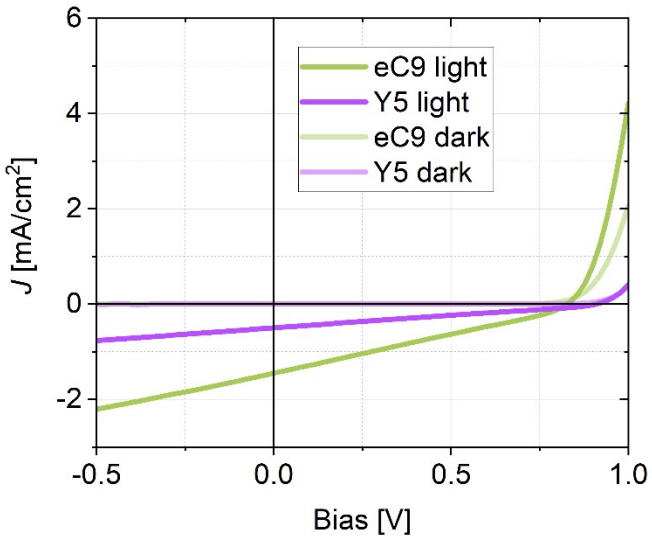

Figure S11: Current density-voltage characteristics of the Y5 and eC9 devices with structure ITO/CuSCN/NFA/Phen-NaDPO/Al (fully reflecting 100nm) with the device area of 6 mm^2 under simulated AM1.5G light in different active layer thickness of 100 nm.

Table S4. Average photovoltaic parameters and standard deviations for NFA devices that are shown in Figure S9. Active layer thickness is ca. 100 nm and A=6 mm^2.

Device	V_{OC} **[V]**	J_{SC} **[mAcm^{-2}]**	**FF [%]**	**PCE [%]**	μ_e **[cm^2/Vs]**	σ_{LUMO} **[meV]**	μ_h **[cm^2/Vs]**	σ_{HOMO} **[meV]**
Y5	0.90	0.96	25	0.2	4×10^{-4}	57	3×10^{-4}	80
eC9	0.82	1.4	26	0.3	1.5×10^{-3}	70	2.5×10^{-8}	85

References

(1) Bruevich, V.; Choi, H. H.; Podzorov, V. The Photo-Hall Effect in High-Mobility Organic Semiconductors. *Adv. Funct. Mater.* **2021**, *31* (7). https://doi.org/10.1002/adfm.202006178.

(2) M, G. L. G.; Bolzonello, L.; Bernal-texca, F. Spatio-Temporal Mapping Uncouples Exciton Diffusion from Singlet-Singlet Annihilation in the Electron Acceptor Y6. 1–21.

(3) Murgatroyd, P. N. Theory of Space-Charge-Limited Current Enhanced by Frenkel Effect. *J. Phys. D. Appl. Phys.* **1970**, *3* (2), 151–156. https://doi.org/10.1088/0022-3727/3/2/308.

(4) Felekidis, N.; Melianas, A.; Kemerink, M. Automated Open-Source Software for Charge Transport Analysis in Single-Carrier Organic Semiconductor Diodes. *Org. Electron.* **2018**, *61*, 318–328. https://doi.org/10.1016/j.orgel.2018.06.010.